0003-4975 https://doi.org/10.1016/j.athoracsur.2025.10.030

Lung: Research

Lymph Node Involvement and Radiologic Predictors of Invasiveness in Pure Ground-Glass Adenocarcinomas: The GORDON Study

Chiara Catelli, MD,[1] Susanna Guerrini, MD,[2] Miriana D'Alessandro, PhD,[3] Maria Antonietta Mazzei, MD,[2] Alfonso Fiorelli, MD, PhD,[4] Lorenzo Rosso, MD, PhD,[5] Mario Nosotti, MD,[5] Giuseppe Marulli, MD, PhD,[6,7] Andrea Dell'Amore, MD,[8] Stefano Margaritora, MD,[9] Beatrice Leonardi, MD,[4] Debora Brascia, MD,[6,7] Federico Rea, MD,[8] Andrea Lloret Madrid, MD,[1] Chiara Giraudo, MD, PhD,[10] Federico Mathieu, MD,[1] Maria Teresa Congedo, MD,[9] Filippo Lococo, MD,[9] and Luca Luzzi, MD,[1] on behalf of the Gordon Study Group*

ABSTRACT

BACKGROUND Pure ground-glass opacities (pGGOs) have been recognized as radiologic manifestations of early-stage lung adenocarcinomas, typically characterized by slow progression and a low risk of metastasis. The study evaluated the incidence of lymph node involvement in patients undergoing pGGO resection. Secondary objectives included assessing lymph node recurrence-free interval and correlating pGGO radiologic features with final histology.

METHODS This multicenter retrospective study (January 2013-June 2024) included patients who underwent pulmonary resection and lymphadenectomy for pGGOs. Data were recorded in the GORDON (Ground-glass Opacities Retrospective Database for Oncological N-status) database. Histologic diagnosis, lymph node involvement, and recurrence were analyzed. Qualitative and quantitative radiologic features of invasive and noninvasive pGGOs were compared, and receiver operating characteristic curve analysis identified predictive variables for invasiveness.

RESULTS Of 400 pGGOs, 346 (86%) were invasive adenocarcinomas, 40 (10%) were minimally invasive, and 14 (4%) were adenocarcinomas in situ. No lymph node metastases were detected. Nodal recurrence at 5 years was 0%. Invasive pGGOs showed larger radiologic diameter (22 vs 16 mm, $P < .001$), higher computed tomographic (CT) attenuation (−336 vs −562 Hounsfield units [HU], $P < .001$), higher difference CT values (−493 vs −313 HU, $P < .001$), and higher relative attenuation ($P < .001$). A combined receiver operating characteristic curve analysis identified a radiologic diameter of 18 mm and CT density of −390 HU as predictive cutoffs for invasiveness (area under the curve, 0.874).

The Supplemental Table can be viewed in the online version of this article [https://doi.org/10.1016/j.athoracsur.2025.10.030] on https://www.annalsthoracicsurgery.org.

Accepted for publication Oct 27, 2025.

*A complete list of members of the GORDON Study Group appears at the end of this article.

Presented at the Thirty-third Annual Conference of the European Society of Thoracic Surgeons, Budapest, Hungary, May 25-27, 2025.

[1]Thoracic Surgery and Lung Transplant Unit, Department of Medicine, Surgery and Neurosciences, Azienda Ospedaliero-Universitaria Senese, University of Siena, Siena, Italy; [2]Diagnostic Imaging Unit, Department of Medicine, Surgery and Neurosciences, Azienda Ospedaliero-Universitaria Senese, University of Siena, Siena, Italy; [3]Respiratory Diseases Unit, Department of Medicine, Surgery and Neurosciences, University of Siena, Siena, Italy; [4]Thoracic Surgery Unit, University of Campania Luigi Vanvitelli, Naples, Italy; [5]Thoracic Surgery and Lung Transplant Unit, Department of Pathophysiology and Transplantation, Fondazione Istituto di Ricovero e Cura a Carattere Scientifico Ca' Granda-Ospedale Maggiore Policlinico, University of Milan, Milan, Italy; [6]Department of Biomedical Sciences, Humanitas University, Milan, Italy; [7]Division of Thoracic Surgery, Istituto di Ricovero e Cura a Carattere Scientifico Humanitas Research Hospital, Humanitas University, Milan, Italy; [8]Division of Thoracic Surgery, Department of Cardiac, Thoracic, Vascular Sciences and Public Health, University of Padua, Padua, Italy; [9]Department of Thoracic Surgery, Fondazione Policlinico Universitario A. Gemelli-Istituto di Ricovero e Cura a Carattere Scientifico, Università Cattolica del Sacro Cuore, Rome, Italy; and [10]Unit of Advanced Clinical and Translational Imaging, Department of Cardiac, Thoracic, Vascular Sciences and Public Health, University of Padua, Padua, Italy

Address correspondence to Dr Catelli, Thoracic Surgery and Lung Transplant Unit, Department of Medicine, Surgery and Neurosciences, University of Siena, Viale Mario Bracci 16, 53100 Siena, Italy; email: chiara.catelli1992@gmail.com.

CONCLUSIONS Adenocarcinomas presenting as pGGOs are low-risk lesions with rare lymph node involvement or recurrence, suggesting that lymphadenectomy may be unnecessary. Preoperative chest CT enables risk stratification of lesion invasiveness, supporting tailored therapeutic approaches.

(Ann Thorac Surg 2025;■:■–■)

Persistent pure ground-glass opacities (pGGOs) identified on chest computed tomography (CT) have been increasingly recognized due to their association with early-stage lung adenocarcinomas.[1] These lesions are typically indolent,[2] with adenocarcinoma in situ (AIS) and minimally invasive adenocarcinoma (MIA) being the least aggressive, with slow progression and minimal metastatic potential.[3]

Hilar and mediastinal lymphadenectomy remains the standard for resectable non-small cell lung cancer, but the low likelihood of nodal involvement in pGGOs—combined with the morbidity of the procedure—warrants reevaluation of its necessity in these cases.

Improved radiologic assessment is essential to estimate pGGO invasiveness and guide surgical decisions, including the need for lymphadenectomy.[4,5]

This study evaluated the incidence of lymph node involvement in surgically resected pGGOs. Secondary objectives include assessing lymph node recurrence and identifying radiologic predictors of histologic invasiveness.

MATERIAL AND METHODS

This multicenter retrospective study included all patients who underwent pulmonary resection with systematic hilar and mediastinal lymphadenectomy for adenocarcinomas presenting as pGGOs between January 2013 and June 2024. The study was conducted in accordance with the Declaration of Helsinki and approved by Siena Institutional Review Board. All patients provided written informed consent for the use of their clinical data for research purposes. We used the Standards for Reporting of Diagnostic Accuracy Studies (STARD) checklist when writing our report.[6]

Data were collected from 6 Italian high-volume oncologic centers. Patient numbers per center are detailed in the Supplemental Table. Each center retrospectively identified all cases of pGGO by reviewing its respective databases of pulmonary resection. In each center, pGGOs were selected for surgical resection according to shared clinical criteria derived from current evidence and guideline recommendations.

The definition for pGGOs was based on types 1 and 2 of the radiologic classification of adenocarcinomas by Suzuki and colleagues,[7] characterized by a homogeneous nodular area of increased lung attenuation, with no solid component visible on CT imaging (both on parenchymal and mediastinal window), through which normal parenchymal structures (airways and vessels) could be visualized.[8]

Exclusion criteria were inadequate lymphadenectomy, lack of preoperative high-resolution CT (HRCT) and contrast-enhanced CT (CECT), inadequate postoperative imaging follow-up, pGGOs >40 mm, history of prior solid lung cancer, and pGGOs developing solid components on preoperative follow-up CT. All participating centers routinely performed lymphadenectomy for resectable non-small cell lung cancer, including pGGO. Although the extent of dissection could vary slightly based on intraoperative judgment, only patients who underwent resection of at least 2 N1 and 2 N2 lobe-specific lymph node stations were included in the analysis.

Eligible cases were entered into the anonymized Ground-glass Opacities Retrospective Database for Oncological N-status (GORDON) database, which includes radiologic and pathologic features and follow-up. No imputation was performed for missing data. Cases with incomplete radiologic or pathologic information were excluded during initial screening.

HISTOPATHOLOGIC EVALUATION AND FOLLOW-UP. The histopathologic examination of surgically resected pGGOs served as the reference standard for this diagnostic accuracy study. For each pGGO, histologic subtype, predominant growth pattern, and pathologic size were recorded. The final histologic diagnosis was based on established criteria, classifying lesions by invasiveness into invasive adenocarcinoma (IAC), MIA, or AIS. To enhance

comparison, 2 groups were defined: IAC and non-IAC (combining MIA and AIS). Lymph node involvement was defined on histopathologic confirmation of pN1 or pN2 disease. Postoperative follow-up included thoracoabdominal CT scans every 6 months for the first 2 years and annually thereafter.

RADIOLOGIC ANALYSIS. Each pGGO underwent detailed radiologic assessment using the most recent HRCT and CECT scans before surgery. CT examinations were acquired with the patient supine using 64-detector row scanners. HRCT was performed in helical mode from lung bases to thoracic inlet, with thin sections (<1 mm), followed by a CECT scan in the late arterial phase (45-50 seconds postcontrast), with breath-hold instructions.

Two experienced clinicians (a radiologist and a thoracic surgeon from each center), blinded to histologic data, reviewed all scans. Nodules were evaluated qualitatively and quantitatively.[9] All assessments were performed on a dedicated workstation using multiplanar reconstruction, with a standardized lung window setting (width, 1500 Hounsfield units [HU]; level, −500 HU).

QUALITATIVE EVALUATION. For each pGGO, location and morphology (rounded/spiculated) were recorded. A pleural tag was defined as ≥1 linear strands extending from the nodule to the pleural surface.[10] Bubble-like lucency referred to round/oval areas of air attenuation within the nodule, whereas the bronchus sign indicated a bronchus entering the lesion on CT.[11] The feeding vessel type (arterial/venous) was also noted; attachment to a pulmonary artery has been associated with invasiveness.[12] In nodules with dual vascular supply, the larger vessel was used for classification.

QUANTITATIVE EVALUATION. Short and long diameters were measured on axial and 2-dimensional multiplanar reconstructions to determine the maximum nodule size. CT attenuation was measured in both unenhanced and postcontrast phases. For unenhanced scans, attenuation was assessed using a lung window (level, −500 HU; width, 1500 HU), placing the region of interest in the most representative part of the GGO, avoiding vessels and bronchi. The same region of interest was copied onto the arterial phase image to ensure consistency. Lung parenchyma attenuation was measured in a region of healthy parenchyma—free of vessels or bronchi—located at least 10 mm from the lesion. This was done on the unenhanced scan using the same lung window settings. The difference in CT values was calculated as the GGO unenhanced CT value minus the lung parenchyma CT value. The relative attenuation was calculated as the ratio of the lung parenchyma CT value to the GGO unenhanced CT value.

STATISTICAL ANALYSIS. Continuous variables are expressed as median and first and third quartile (interquartile range (IQR]). Categorical variables are expressed as number (percentages). Nonparametric tests were used for group comparisons: the Mann-Whitney *U* test for 2 groups and the Kruskal-Wallis test with the Dunn post hoc correction for comparisons among>2 groups. Categorical variables were analyzed using contingency tables to assess associations and independence between variables. Kaplan-Meier analysis was used to estimate lymph node recurrence-free interval (LNRFI) at 1, 3, and 5 years, with censoring of patients without recurrence. Binomial logistic regression analysis was performed to determine any significant effects of IAC with respect to the control group (explanatory variables: IAC vs non-IAC) considered in interaction or otherwise with round margins, percentage of acinar, lepidic, papillary component, radiologic tumor size, GGO unenhanced and postcontrast CT attenuation, and bubble-like lucency as dependent variables. The null hypothesis, which excludes any effect of the explanatory variable on the combination of dependent variables (ie, that IAC has no effect on the dependent variables, with a very small risk of being wrong) was assessed. All statistical analyses were conducted using GraphPad Prism 9.10.3 software (GraphPad Software) and Jamovi software. A *P* value <.05 was considered statistically significant.

RESULTS

Between January 2013 and June 2024, 474 pulmonary resections for adenocarcinomas presenting as pGGOs were performed across 6 participating centers. We excluded 37 cases due to lack of intraoperative lymphadenectomy, 30 for inadequate preoperative CT, 4 for lesion size >40 mm, and 3 for prior solid lung cancer, resulting in 400 eligible pGGOs (Figure 1).

Of these, 211 (52.8%) were from female patients. Patients were a mean age of 67.5 (SD, 8.9) years. Radiologic and pathologic features are

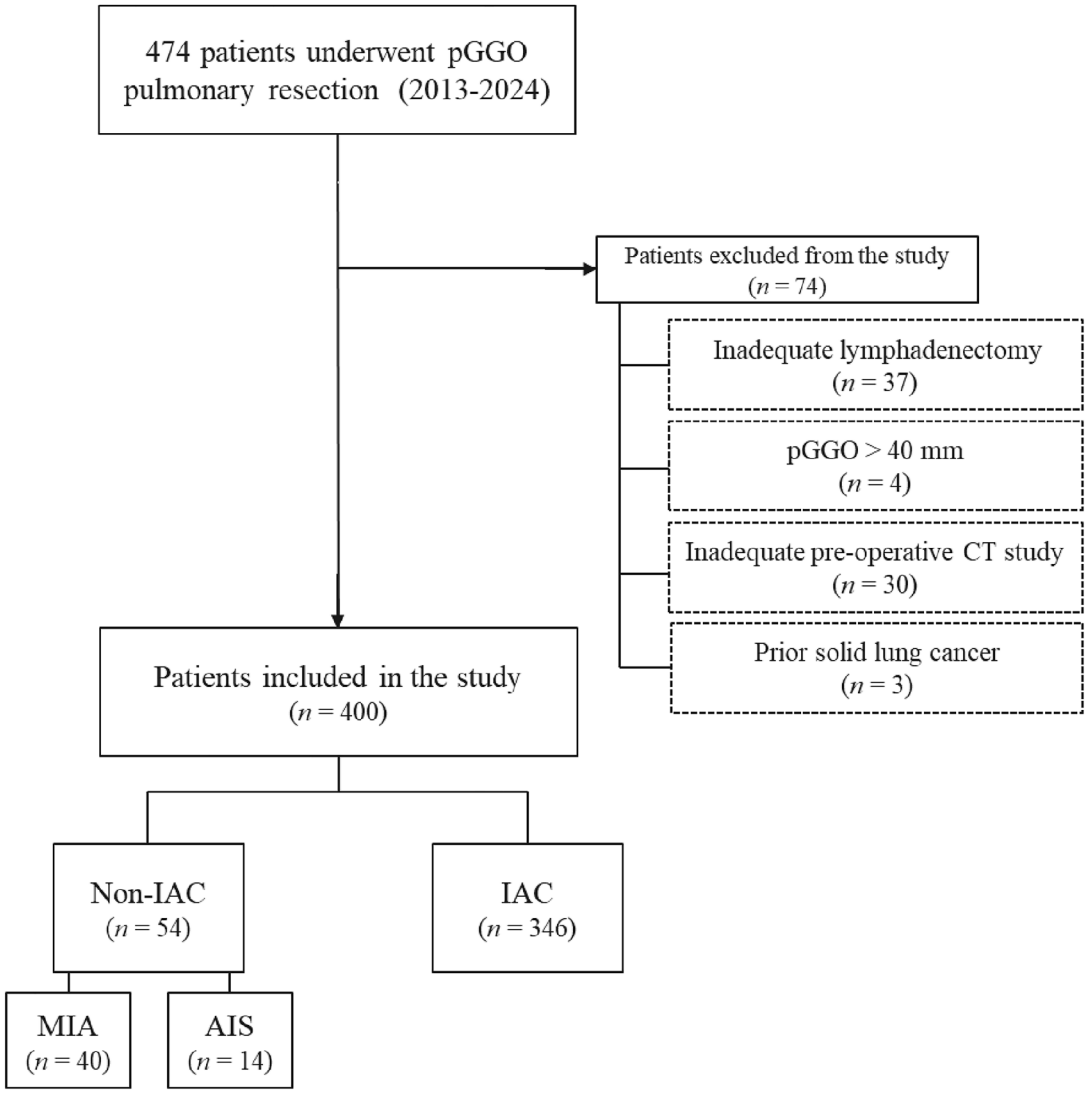

FIGURE 1 Flowchart of patient selection and histologic classification. (AIS, adenocarcinoma in-situ; CT, computed tomography; IAC, invasive adenocarcinoma; MIA, minimally invasive adenocarcinoma; pGGO, pure ground-glass opacity.)

detailed in Table 1. Most nodules were in the upper lobes (273 [68.2%]). Mean radiologic maximum diameter was 21.9 (SD, 8.8) mm. All lesions were staged as cN0. Radiologically, 218 nodules (54.6%) had smooth margins, 263 (65.9%) showed pleural tags, 103 (25.9%) had bubble-like lucency, and 183 (45.9%) had a bronchus sign. Arterial vascularization was observed in 230 cases (58.2%). Mean GGO unenhanced CT attenuation was −367 HU (range, −496 to −226 HU), and GGO arterial phase attenuation was −405 HU (range, −566 to −182 HU). The median difference CT value was −473 HU (IQR, −617 to −342 HU), and relative attenuation averaged 2 (range, 2-3).

Lobectomy was performed in 65.5% of cases, segmentectomy in 26.0%, and atypical resection in 8.5%. Histology revealed 346 IACs (86.4%) and 54 non-IACs (40 MIA [10.0%] and 14 AIS [3.5%]). Lobectomy was significantly more frequent in patients with IAC (68.5%) compared with those with AIS or MIA (46.3%, $P = .005$). Mean pathologic maximum diameter was 17.7 mm (SD, 7.9 mm). Among IACs, 80 (23.1%) were pT1a, 123 (35.5%) were pT1b, 51 (14.7%) were pT1c, and 92 (26.6%) were pT2, including 36 with visceral pleural invasion. The predominant growth patterns were acinar (50.3%), lepidic (39.4%), and papillary (7.7%). A mean of 6.3 (SD, 5.1) lymph nodes was resected from N1 stations and 5.6 (SD, 5.3) from N2 stations. All specimens

TABLE 1 Pure Ground-Glass Opacity Radiologic and Anatomopathologic Characteristics and Comparison Between Invasive Adenocarcinomas and Minimally Invasive or In Situ Adenocarcinomas (non-IACs)

Variables	Total (N = 400)	IAC (n = 346)	Non-IAC (n = 54)	*P*
Age, y	69 (62 to 74)	69 (62 to 74)	67 (60 to 72)	.17
Female sex	211 (52.8)	182 (52.6)	29 (53.7)	.88
Location				.54
Right upper lobe	167 (41.8)	152 (43.9)	15 (27.8)	
Left upper lobe	106 (26.4)	89 (25.7)	17 (31.2)	
Right middle lobe	15 (3.8)	12 (3.5)	3 (5.6)	
Right lower lobe	66 (16.5)	54 (15.6)	12 (22.2)	
Left lower lobe	46 (11.4)	39 (11.3)	7 (13.0)	
Radiologic tumor size, mm	21 (15 to 27)	22 (16 to 28)	16 (12 to 22)	<.001
cN0 stage	400 (100)	346 (100)	54 (100)	>.99
Round margins	218 (54.6)	179 (51.7)	39 (72.2)	.005
Pleural tag	263 (65.9)	238 (68.8)	25 (46.3)	.001
Bubble-like lucency	103 (25.9)	92 (26.6)	11 (20.4)	.36
Bronchus sign	183 (45.9)	165 (47.7)	18 (33.3)	.05
Arterial vascularization	230 (58.2)	201 (58.1)	29 (53.7)	.08
GGO unenhanced CT attenuation, HU	−367 (−496 to −226)	−336 (−450 to −200)	−562 (−638 to −447)	<.001
GGO arterial CT attenuation, HU	−405 (−566 to −182)	−330 (−488 to −68)	−567 (−611 to −440)	<.001
Difference CT value, HU	−473 (−617 to −342)	−493 (−635 to −383)	−313 (−404 to −241)	<.001
Relative attenuation, mean (SD)	2.85 (15.78)	3.04 (17.2)	1.72 (0.69)	<.001
Type of lung resection				.005
Lobectomy	262 (65.5)	237 (68.5)	25 (46.3)	
Segmentectomy	104 (26.0)	83 (24.0)	21 (38.9)	
Atypical resection	34 (8.5)	26 (7.5)	8 (14.8)	
Resected lymph nodes, n				
N1	5 (1 to 10)	6 (2 to 10)	3 (1 to 8)	.02
N2	4 (2 to 8)	4 (2 to 8)	3 (2 to 5)	.01
Prevalent growth pattern				<.001
Acinar	211 (52.7)	209 (60 to 4)	2 (3.7)	
Lepidic	147 (36.8)	95 (27.5)	52 (96.3)	
Papillary	25 (6.2)	25 (7.2)	0	
Other	17 (4.3)	17 (4.9)	0	
Anatomopathologic tumor size, mm	17 (12 to 22)	18 (12 to 24)	12 (9 to 15)	<.001
T stage				
0	54 (13.6)	…	…	
1a	80 (20.0)	…	…	
1b	123 (30.8)	…	…	
1c	51 (12.8)	…	…	
2a	92 (23.0)	…	…	
N stage				
0	400 (100)	346 (100)	54 (100)	1.000
Recurrence	1 (0.2)	1 (0.3)	0	.998

Data are shown as n (%) for categorical variables and as median (first, third quartile) for continuous variables or as indicated otherwise as mean (SD). *P* value indicates the comparison between IAC and non-IAC. CT, computed tomography; GGO, ground-glass opacity; HU, Hounsfield units; IAC, invasive adenocarcinoma.

were pN0. Median follow-up was 30 months (IQR, 18-35 months). LNRFI was 100% at 1, 3, and 5 years.

One patient experienced recurrence 76 months after lobectomy. The original lesion was a spiculated pGGO with high-risk features: maximum radiologic diameter of 33 mm, pleural tag, arterial vascularization, bubble-like lucency, and bronchus sign. CT attenuation metrics showed an unenhanced CT value of −80 HU, a difference CT value of −586 HU, and a relative attenuation of 3.03. Histologically, the tumor was an IAC, pT2a, with 100% acinar pattern. The recurrence involved lymph nodal 4R station only. The patient was treated with systemic therapy and remained alive at the last follow-up.

COMPARATIVE ANALYSIS BETWEEN IACS AND MIACS OR NON-IACS. The comparative analysis results (focused primarily on radiologic features derived from preoperative CT scans) (Figure 2) are presented in Table 1. No significant differences were found between IAC and non-IAC groups regarding age, sex, or lesion location. pGGOs in the IAC group were significantly larger (22 mm [IQR, 16-28 mm] vs 16 mm [IQR, 12-22 mm], $P < .001$). Smooth margins were more common in non-IACs (72.2% vs 51.7%, $P = .005$), whereas pleural tags (68.8% vs 46.3%, $P = .001$) and the bronchus sign (47.7% vs 33.3%, $P = .05$) were more frequent in IACs. Arterial-dominant vascularization was slightly more prevalent in IACs (58.1% vs 53.7%) but not statistically significant ($P = .08$). CT attenuation values were significantly higher (less negative) in IACs. Median attenuation in the unenhanced phase

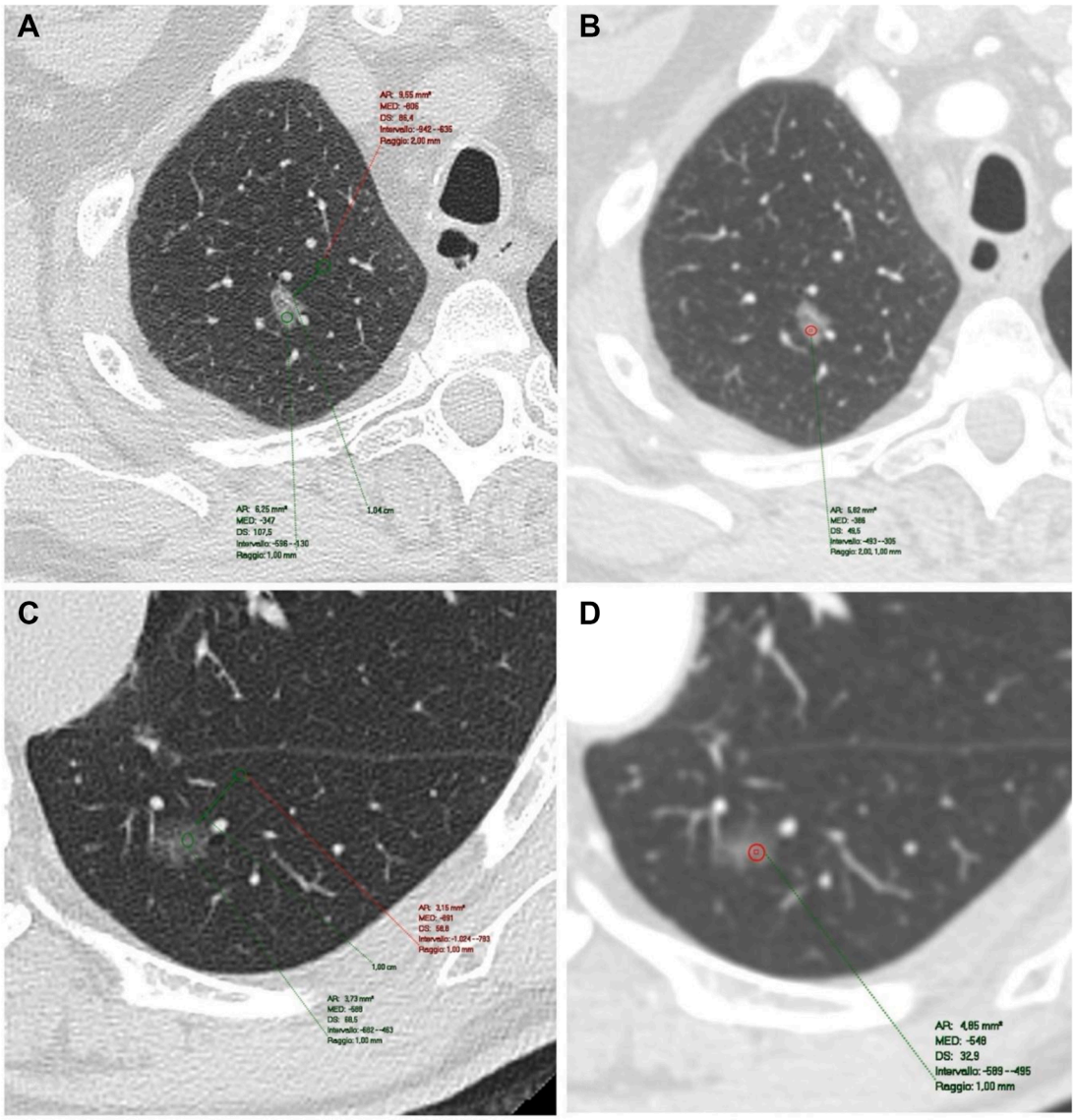

FIGURE 2 Radiologic evaluation in preoperative computed tomography (CT) scan. The upper images show the (a) unenhanced and the (b) postcontrast CT acquisitions of an invasive adenocarcinoma (IAC), whereas the lower images display the (c) unenhanced and (d) postcontrast phases of an adenocarcinoma in situ (AIS). The region of interest in the nodule highlights the differences in density between IAC and non-IAC both in the unenhanced (a: −347 Hounsfield units [HU] vs c: −588 HU) and postcontrast phase (b: −386 HU vs d: −548 HU). In images a and c, an additional region of interest is placed in the surrounding normal parenchyma to obtain the parenchyma attenuation necessary for the calculation of the difference CT value and relative attenuation.

was −336 HU (IQR, −450 to −200 HU) in IACs vs −562 (IQR, −638 to −477 HU) in non-IACs ($P <$ .001); and in the arterial phase was -330 HU (IQR, −488 to −68 HU) vs -567 HU (IQR, −611 to −440 HU) ($P <$ .001). The difference CT value was higher in IACs (-493 HU [IQR, −635 to −383 HU] vs −313 HU (IQR, −404 to −241 HU], $P <$ .001), whereas relative attenuation was higher (3.04 [SD, 17.2] vs 1.72 [SD, 0.69], $P <$ .001), reflecting greater contrast with surrounding lung parenchyma.

Receiver operating characteristic (ROC) curve analysis was conducted on quantitative radiologic variables from unenhanced CT scans to identify predictors of pGGO invasiveness (Figure 3). For maximum lesion diameter, the highest odds ratio (OR) of 0.906 was observed at a 17.9 mm cutoff, with 59.3% specificity, 69.0% sensitivity, and area under the curve (AUC) of 0.679 (95% CI, 0.6027-0.7542; $P <$ .0001). Unenhanced CT attenuation showed the highest OR of 0.991 at −390 HU, with 92.6% specificity, 63.9% sensitivity, and AUC of 0.383 (95% CI, 0.7878-0.8874; $P <$ .0001). The optimal cutoff for the difference CT value was -411 HU (OR, 1.001), yielding 85.2% specificity, 70.5% sensitivity, and AUC of 0.803 (95% CI, 0.7562-0.8490; $P <$ .0001). For relative attenuation, the best cutoff was 1.8 (OR, 0.992), with 72.5% specificity, 70.4% sensitivity, and AUC of 0.778 (95% CI, 0.7300-0.8249; $P <$ .0001).

The combined ROC curve analysis (Figure 4), incorporating all 4 variables demonstrated that only radiologic diameter >18 mm ($P <$ .001) and unenhanced attenuation exceeding −390 HU ($P =$ .03) were significant independent predictors of invasiveness. Although the difference CT value and relative attenuation were both significantly associated with invasive adenocarcinoma in univariate ROC curve analysis ($P <$ .001), they did not retain statistical significance in the combined multivariable model ($P =$ .82 and $P =$ .90, respectively). The combined model yielded 75.9% sensitivity, 82.0% specificity, 81.2% overall accuracy, and an AUC of 0.874.

COMMENT

This multicenter study analyzed 400 cases of surgically resected pGGOs confirmed as primary lung adenocarcinomas. To our knowledge, this represents one of the largest multicenter cohorts specifically focused on lymph node involvement and radiologic predictors of invasiveness in adenocarcinomas presenting exclusively as pGGOs.

Notably, no nodal metastases were identified, even among the 346 cases (86%) of IAC. LNRFI was 100% at 1, 3, and 5 years. These findings strongly support the view that pGGOs—despite frequent invasive histology—represent a

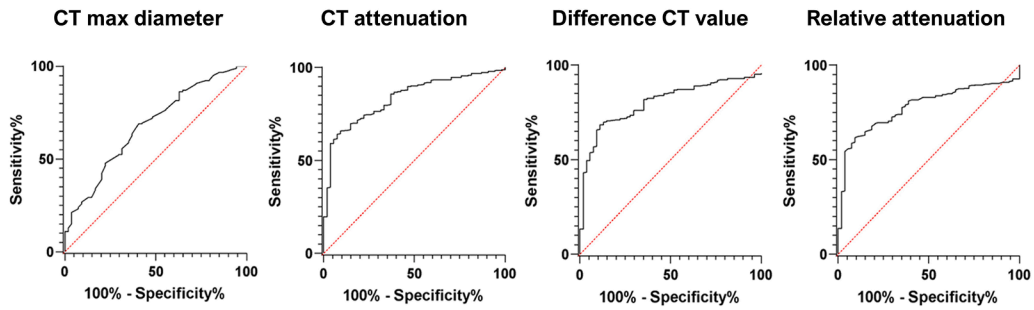

	CT max diameter	CT attenuation	Difference CT value	Relative attenuation
Area Under the Curve (%)	67.8 (95%CI 60.2 – 75.4)	83.8 (95%CI 78.8 – 88.7)	80.3 (95%CI 75.6 – 84.9)	83.8 (95%CI 73 – 82.5)
P value	<0.0001	<0.0001	<0.0001	<0.0001
Cut-off	18	-390.5	-411	-1.8
Sensitivity (%)	69	63.9	70.5	72.5
Specificity (%)	59.3	92.6	85.2	70.4

FIGURE 3 Single receiver operating characteristic curve analyses to identify cutoff values for predicting ground-glass opacity invasiveness. Receiver operating characteristic curves showing diagnostic performance of individual computed tomographic (CT) variables in distinguishing invasive from noninvasive pure ground-glass opacities.

Combined Receiver Operating Characteristics curve analysis – IAC vs. non-IAC							
Predictor	Estimate	SE	Z	p	Odds ratio	95% Confidence Interval	
						Lower	Upper
Intercept	-3.00530	3.05835	-0.983	0.326	0.0495	1.23e-4	19.865
Difference CT value	8.52e-4	0.00372	0.229	0.819	1.0009	0.994	1.008
Relative attenuation	-0.00845	0.06743	-0.125	0.900	0.9916	0.869	1.132
CT max diameter	-0.09808	0.02429	-4.038	**<.001**	0.9066	0.864	0.951
CT unenhanced attenuation	-0.00785	0.00352	-2.233	**0.026**	0.9922	0.985	0.999

Estimates represent the log odds of "IAC vs non-IAC = non-IAC" vs. "IAC vs non-IAC = IAC"; CT: Computed Tomography; SE: standard Error

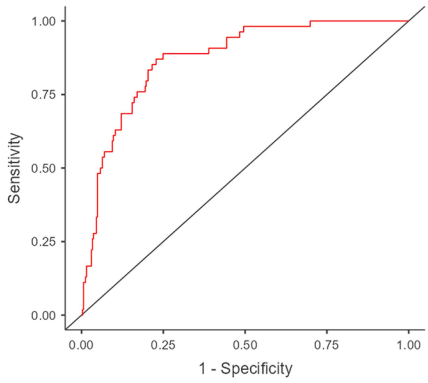

Predictive Measures			
Accuracy	Specificity	Sensitivity	AUC
0.812	0.820	0.759	0.874

FIGURE 4 Combined receiver operating characteristic curve analysis to predict the pure ground-glass opacity invasiveness. (CT, computed tomography; IAC, invasive adenocarcinoma.)

biologically indolent cancer subtype with extremely low metastatic potential. Our results are in line with previous studies reporting minimal nodal involvement in pure GGOs,[13,14] raising questions about routine systematic lymphadenectomy. Given the potential morbidity associated with lymphadenectomy (bleeding, chylothorax, and nerve injury), its omission in selected patients could be both safe and beneficial.

In addition, our study highlights key radiologic predictors of histologic invasiveness. ROC curve analysis demonstrated that a diameter ≥18 mm and an unenhanced CT value exceeding −390 HU accurately predicted invasiveness (sensitivity, 75.9%; specificity, 82.0%; AUC, 0.874), in agreement with prior evidence supporting the prognostic role of size and density.[15] Interestingly, the difference CT value and relative attenuation both demonstrated a significant association with invasiveness in the univariate ROC curve analysis, supporting their potential relevance in distinguishing IAC from non-IAC. However, when these variables were evaluated within the combined multivariable ROC curve model, their predictive power was no longer statistically significant, their influence being likely redundant with stronger predictors such as size and CT attenuation.

CECT attenuation was also significantly higher in IACs than in non-IACs, suggesting that contrast enhancement may reflect increased vascularity associated with invasiveness. These findings support the role of CECT as a valuable adjunct to HRCT in preoperative assessment and risk stratification. Lastly, qualitative well-known features, such as spiculated margins,[16] pleural tags, and bronchus sign, were significantly more frequent in invasive lesions, suggesting subtle invasive behavior beyond size and density. These features may aid surgical planning and risk evaluation, especially in borderline cases.

Our cohort reveals marked differences compared with findings reported in Asian series, such as those by Li and colleagues[4] and Eguchi and colleagues.[15] Whereas in their studies ∼74% to 78% of pGGOs were classified as AIS or MIA, 86.4% of lesions in our population were IAC. This discrepancy may reflect underlying biological differences in tumor behavior between populations, or alternatively, a more conservative surgical approach adopted by our centers when selecting pGGOs for resection.

A comparison with the recent randomized controlled trial by Zhang and colleagues[17] is valuable but must be contextualized. Unlike their trial, which included only IACs with a consolidation tumor ratio ≤0.5, our study included both invasive and noninvasive pGGOs. The inclusion of non-IACs aimed to explore imaging features predictive of invasiveness—potentially supporting preoperative decision-making on which lesions to refer for surgery—an aspect not addressed by Zhang and collueagues,[17] who focused solely on the necessity of mediastinal lymph node dissection.

Our study included both anatomical and nonresections; however, no lymph node involvement

was observed in any subgroup, indicating that the type of surgical resection, when radical, does not impact nodal status. Lastly, our cohort was limited to pGGOs, excluding GGO-dominant lesions with solid components; thus, consolidation tumor ratio was not a relevant variable, and we applied a broader inclusion threshold of ≤40 mm to better reflect real-world clinical practice.

In the current landscape, artificial intelligence and radiomics are rapidly advancing in imaging, offering great promise, but requiring specialized software. In contrast, the variables identified in our study are readily accessible using standard imaging software available in most clinical settings, and obtainable quickly and reliably by radiologists or clinicians during routine image review. As such, they offer a practical, cost-effective means of stratifying risk and guiding surgical planning, making them suitable for widespread clinical adoption.

CLINICAL IMPLICATIONS.

Precision resection strategy. In our study, we observed a high proportion of lobectomies for non-IACs, which raises concerns about potential overtreatment. Given the simplicity and reproducibility of the invasiveness predictors analyzed, in pGGOs with a diameter ≥18 mm and density exceeding −390 HU, a more extensive surgical approach may be justified against a potentially invasive disease, whereas lesions below these thresholds may be suitable for sublobar resection, without compromising oncologic safety. Given the absence of nodal involvement and the excellent LNRFI observed in our cohort, the routine use of lymphadenectomy in pGGOs may be unnecessary, potentially reducing operative morbidity and surgery time.

Guiding follow-up and surveillance. As lung cancer screening becomes widespread,[18] incidental detection of pGGOs is increasing. Monitoring for changes in size (growth >18 mm) or attenuation (crossing the −390 HU threshold) during serial imaging can help identify lesions progressing toward invasiveness. In fact, part-solid nodules frequently evolve from pGGOs, representing a natural continuum in tumor aggressiveness. Although this progression rarely results in unresectability due to the typically slow growth rate, it is associated with worse prognosis and thus warrants timely intervention.[19] Incorporating these thresholds into follow-up protocols may refine risk stratification and surgical timing.

Management of multiple GGOs. In patients presenting with multiple GGOs, our findings offer a practical approach to lesion prioritization. Applying the identified radiologic criteria allows clinicians to target nodules with the highest probability of invasiveness, thereby optimizing treatment plans. This individualized strategy aligns with current recommendations advocating tailored management based on lesion-specific characteristics.

LIMITATIONS. This study presents several limitations. First, its retrospective design may introduce selection and information bias. Another limitation is the lack of a standardized surgical indication protocol across participating centers. Although all institutions applied consistent radiologic criteria for identifying pGGO, the decision to proceed with surgery may have been influenced by local expertise and clinical judgment. Moreover, the exclusive inclusion of surgically resected pGGOs precludes direct evaluation of the natural history of lesions managed with active surveillance.

CONCLUSIONS. pGGOs, even when invasive, carry minimal risk of lymph node involvement or recurrence. These findings support a paradigm shift toward de-escalation of lymphadenectomy in patients with pGGOs, ultimately reducing surgical morbidity without compromising oncologic efficacy. Simple and reproducible CT measurements—particularly lesion size and attenuation—provide a strong predictive value for histologic invasiveness and may guide a more individualized surgical approach.

The GORDON Study Group: Chiara Catelli, Floriana Barra, Miriana D'Alessandro, Cristiana Bellan, Piero Paladini, Luca Luzzi, Andrea Lloret Madrid, Susanna Guerrini, Maria Antonietta Mazzei, Lorenzo Rosso, Mario Nosotti, Margherita Brivio, Gianluca Lopez, Andrea Dell'Amore, Chiara Giraudo, Alessandro Bonis, Sara Cecchinato, Anna Michielin, Filippo Lococo, Stefano Margaritora, Giuseppe Calabrese, Maria Teresa Congedo, Anna Rita Larici, Marica Andrisani, Paolo Mendogni, Valentina Vespro, Alfonso Fiorelli, Beatrice Leonardi, Riccardo Monti, Giuseppe Marulli, Debora Brascia, and Veronica Giudici.

FUNDING SOURCES

The authors have no funding sources to disclose.

DISCLOSURES

The authors have no conflicts of interest to disclose.

REFERENCES

1. Kim HY, Shim YM, Lee KS, et al. Persistent pulmonary nodular ground-glass opacity at thin-section CT: histopathologic comparisons. *Radiology*. 2007;245:267–275. https://doi.org/10.1148/radiol.2451061682. Published correction appears in *Radiology*. 2008;247:297.

2. Zhang Y, Fu F, Chen H. Management of ground-glass opacities in the lung cancer spectrum. *Ann Thorac Surg*. 2020;110:1796–1804. https://doi.org/10.1016/j.athoracsur.2020.04.094

3. Henschke CI, Yankelevitz DF, Mirtcheva R, et al. ELCAP Group. CT screening for lung cancer: frequency and significance of part-solid and nonsolid nodules. *AJR Am J Roentgenol*. 2002;178:1053–10457. https://doi.org/10.2214/ajr.178.5.1781053

4. Li D, Deng C, Wang S, et al. Ten-year follow-up results of pure ground-glass opacity-featured lung adenocarcinomas after surgery. *Ann Thorac Surg*. 2023;116:230–237. https://doi.org/10.1016/j.athoracsur.2023.01.014

5. Yotsukura M, Asamura H, Motoi N, et al. Long-term prognosis of patients with resected adenocarcinoma in situ and minimally invasive adenocarcinoma of the lung. *J Thorac Oncol*. 2021;16:1312–1320. https://doi.org/10.1016/j.jtho.2021.04.007

6. Bossuyt PM, Reitsma JB, Bruns DE, et al. STARD 2015: an updated list of essential items for reporting diagnostic accuracy studies. *BMJ*. 2015;351:h5527. https://doi.org/10.1136/bmj.h5527

7. Suzuki K, Kusumoto M, Watanabe S, et al. Radiologic classification of small adenocarcinoma of the lung: radiologic-pathologic correlation and its prognostic impact. *Ann Thorac Surg*. 2006;81:413–419. https://doi.org/10.1016/j.athoracsur.2005.07.058

8. Bankier AA, MacMahon H, Colby T, et al. Fleischner Society: glossary of terms for thoracic imaging. *Radiology*. 2024;310:e232558. https://doi.org/10.1148/radiol.232558

9. Qi L, Xue K, Li C, et al. Analysis of CT morphologic features and attenuation for differentiating among transient lesions, atypical adenomatous hyperplasia, adenocarcinoma in situ, minimally invasive and invasive adenocarcinoma presenting as pure ground-glass nodules. *Sci Rep*. 2019;9:14586. https://doi.org/10.1038/s41598-019-50989-1

10. Meng Y, Gao J, Wu C, et al. The prognosis of different types of pleural tags based on radiologic-pathologic comparison. *BMC Cancer*. 2022;22:919. https://doi.org/10.1186/s12885-022-09977-4

11. Chu ZG, Li WJ, Fu BJ, Lv FJ. CT Characteristics for predicting invasiveness in pulmonary pure ground-glass nodules. *AJR Am J Roentgenol*. 2020;215:351–358. https://doi.org/10.2214/AJR.19.22381

12. Barnett J, Pulzato I, Wilson R, et al. Perinodular vascularity distinguishes benign intrapulmonary lymph nodes from lung cancer on computed tomography. *J Thorac Imaging*. 2019;34:326–328. https://doi.org/10.1097/RTI.0000000000000394

13. Lin YH, Chen CK, Hsieh CC, et al. Lymphadenectomy is unnecessary for pure ground-glass opacity pulmonary nodules. *J Clin Med*. 2020;9:672. https://doi.org/10.3390/jcm9030672

14. Moon Y, Sung SW, Namkoong M, Park JK. The effectiveness of mediastinal lymph node evaluation in a patient with ground glass opacity tumor. *J Thorac Dis*. 2016;8:2617–2625. https://doi.org/10.21037/jtd.2016.08.75

15. Eguchi T, Yoshizawa A, Kawakami S, et al. Tumor size and computed tomography attenuation of pulmonary pure ground-glass nodules are useful for predicting pathological invasiveness. *PLoS One*. 2014;9:e97867. https://doi.org/10.1371/journal.pone.0097867

16. Catelli C, Guerrini S, D'Alessandro M, et al. Sarcoid nodule or lung cancer? A high-resolution computed tomography-based retrospective study of pulmonary nodules in patients with sarcoidosis. *Diagnostics (Basel)*. 2024;14:2389. https://doi.org/10.3390/diagnostics14212389

17. Zhang Y, Qian B, Song Q, et al. Phase III study of mediastinal lymph node dissection for ground glass opacity-dominant lung adenocarcinoma. *J Clin Oncol*. 2025;43:3081–3089. https://doi.org/10.1200/JCO-25-00610

18. Bonney A, Malouf R, Marchal C, et al. Impact of low-dose computed tomography (LDCT) screening on lung cancer-related mortality. *Cochrane Database Syst Rev*. 2022;8:CD013829. https://doi.org/10.1002/14651858.CD013829.pub2

19. Kakinuma R, Noguchi M, Ashizawa K, et al. Natural history of pulmonary subsolid nodules: a prospective multicenter study. *J Thorac Oncol*. 2016;11:1012–1028. https://doi.org/10.1016/j.jtho.2016.04.006